Energy flow in light-coupling masks for lensless optical lithography

Olivier J. F. Martin and Nicolas B. Piller

Electromagnetic Fields and Microwave Electronics Laboratory Swiss Federal Institute of Technology, ETH-Zentrum, ETZ 8092 Zurich, Switzerland

martin@ifh.ee.ethz.ch

Heinz Schmid, Hans Biebuyck and Bruno Michel

IBM Research Division, Zurich Research Laboratory 8803 Rüchlikon, Switzerland

sih@zurich.ibm.com

Abstract: We illustrate the propagation of light in a new type of coupling mask for lensless optical lithography. Our investigation shows how the different elements comprising such masks contribute to the definition of an optical path that allows the exposure of features in the 100-nm-size range in the photoresist.

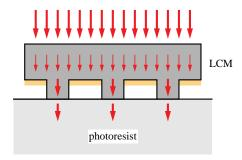
©1998 Optical Society of America

OCIS codes: (050.1220) Apertures; (110.3960) Microlithography; (110.5220) Photolithography; (220.3740) Lithography; (220.4000) Microstructure fabrication; (230.4000) Microstructure fabrication; (260.2110) Electromagnetic theory; (290.0290) Scattering; (350.3950) Micro-optics

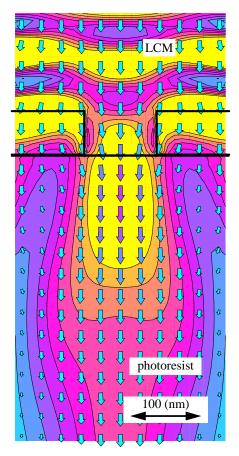
References and links

- H. Schmid, H. Biebuck, B. Michel and O.J.F. Martin, "Light-coupling masks for lensless, subwavelength optical lithography," Appl. Phys. Lett. 72, 2379–2381 (1998).
- 2. H. Schmid, H. Biebuck, B. Michel, O.J.F. Martin and N.B. Piller, "Light-coupling masks: an alternative, lensless approach to high-resolution optical contact lithography," J. Vac. Sci. Technol. B in press (1998).
- 3. Special issue on optical lithography, IBM J. Res. Develop. 41(1/2) (1997).
- H.A. Biebuyck, N.B. Larsen, E. Delamarche and B. Michel, "Lithography beyond light: microcontact printing with monolayer resists," IBM J. Res. Develop. 41, 159–170 (1997).
- N.B. Piller and O.J.F. Martin, "Increasing the performances of the coupled-dipole approximation: A spectral approach," IEEE Trans. Antennas Propag. 46, 1126–1137 (1998).
- O.J.F. Martin and N.B. Piller, "Electromagnetic scattering in polarizable backgrounds," Phys. Rev. E 58, 3909–3915 (1998).
- 7. Olivier J.F. Martin home page: http://www.ifh.ee.ethz.ch/~martin
- 8. IBM Zurich Research Laboratory home page: http://www.zurich.ibm.com

We recently introduced a new approach to optical contact lithography based on polymer light-coupling masks (LCMs) [1,2]. The surface of such a mask is molded so that the areas to be exposed in the photoresist form protrusions on the mask surface (Fig. 1). Thus when an LCM is placed in conformal contact with a photoresist, mechanical contact between mask and photoresist occurs only in the regions to be exposed. The mask is illuminated from its backside and the optical energy is guided through the contacting areas of the mask and coupled into the photoresist (Fig. 1).



Schematic view of a light-coupling mask (LCM) and its operation. The areas to be exposed in the photoresist correspond to protrusions on the mask surface, to which the light is guided. A thin gold layer can be deposited on the noncontacting portions of the mask to enhance the contrast.



Light propagation through an LCM defined only by air gaps. The width of the protrusion is $100\,\mathrm{nm}$ and its height $60\,\mathrm{nm}$. The figure shows the field intensity map and the Quicktime movie an animation of the field propagation in the structure (evolution of the electric field amplitude as a function of time; each frame represents a 10° change in the phase of the field). The arrows represent the time-averaged Poynting vector.

The lateral air gaps that circumscribe the protrusions in the mask act as enhancing elements for the field because the light tends to propagate along paths of constant polarizability (i.e. through the protrusions) and to be reflected back at the mask/air interfaces. Light leaking through the noncontacting portions of the mask can be further suppressed by the addition of a metallic adsorber (Fig. 1).

We made features as small as 100 (nm) on a 200 (nm) pitch in photoresist. With this technique, comparatively large areas (>10 cm²) can, in addition, be exposed at these resolutions in a single step [1]. This approach is therefore an alternative to conventional lithography based on diffractive optics [3].

Several distinctive features of LCMs contribute to their performance. First, the optical index of the polymer (n = 1.6 for a UV wavelength of λ = 248 (nm)) significantly reduces the effective wavelength in the mask. Second, the relatively close match between the refractive index of the mask and the photoresist minimizes undesired scattering of light where they contact. Third, the ability of LCMs to guide the light selectively towards the contacting area provides high contrast and efficient exposures. Fourth, the elastomeric properties of LCMs allow conformal mechanical contact without damaging the mask so that many cycles of exposure through it are possible.

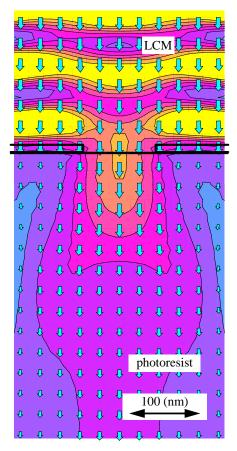


Fig. 3. Contribution of a 10-nm-thick gold layer to the light propagation in an LCM. The figure shows the field intensity map and the Quicktime movie an animation of the field propagation in the structure (evolution of the electric field amplitude as a function of time; each frame represents a 10° change in the phase of the field). The arrows represent the time-averaged Poynting vector.

This conformal contact between mask and photoresist is mandatory for achieving high resolution lithography. Indeed, a non-ideal contact leads to lateral light leakages that broaden the exposed region. The fabrication of the organic mask from a structured master, made by electron-beam lithography, represents therefore the key point for this technology. It has been described in detail in Refs. [1,2,4].

The resolution limit of this new type of optical lithography is discussed extensively in Ref. 1. The objective of the present article is to illustrate how energy flows in LCMs and to elucidate the role of the different optical components that constitute the mask. When the size of their elements is similar to the effective wavelength in the media, it is not possible to rely simply on ray or far-field optics to investigate LCMs. Instead, we use a more complete description of the scattering at the nanoscale to analyze the behavior of the field and its propagation in such a system.

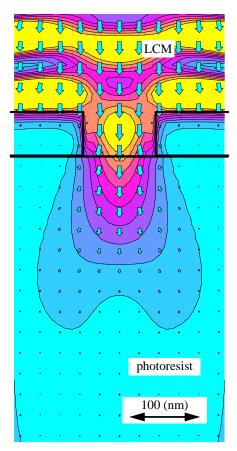


Fig. 4. Same situation as in Fig. 3, but for a 60-nm-thick gold layer.

For the simulations presented in this paper we used the filtered coupled-dipole approximation that assumed a polarizable background [5,6]. This fully vectorial technique provides an accurate, self-consistent solution to the light-scattering problem. As the LCM and photoresist are in effect index-matched for our purposes, we simply considered an infinite, homogeneous background with a refractive index of 1.6, discretizing only the air gaps and metal layers that define the protrusion. The calculations were fully three-dimensional, although we only present cuts through the LCM structure here. In particular, the lateral extension of the air gaps and metal layer was 300 (nm) in both directions in our simulations. The vacuum wavelength was $\lambda = 248$ (nm) and its inci-

dent polarization on the mask was circular. We use the same color scale (from light blue to yellow, highest, in 10% increments of intensity) for the various figures and films presented in this article to facilitate their comparison.

Figure 2 illustrates the propagation of the field through an LCM formed only from polymer, i.e. without the presence of an additional metallic adsorber. In this configuration, the energy is simply guided through the protrusions, whereas the lateral air gaps, which have a much lower index than the surrounding polymer, act like divergent lenses that focus the field towards the center of the coupling area. The latter is particularly evident from the angle of the Poynting vectors at the lower edges of the protrusion. Strong back-reflections of the incident field are also present, leading to stationary waves above the structure. The field intensity in the air gaps remains significant, and some energy passes through the mask into the photoresist, lowering the achievable contrast.

Contrast can be enhanced by the selective deposition of a thin metal layer on an LCM. How such a layer influences the energy flow in the mask is first illustrated in Fig. 3 for a simpler case, where we show the propagation of light through a 10-nm-thick gold layer embedded in a polymer but having no air gaps. The permittivity of gold is $\varepsilon = -0.87 + i4.31$ at this wavelength, so most of the incident field is absorbed in the metal, greatly reducing the degree of backscattering compared to the case shown in Fig. 2. The contrast is weak in the forward direction, however, and the energy flow into the photoresist appears quite homogeneous. A small divergence of the field appears just at the edges of the coupling region that is even more pronounced in simulations of thicker layers of metal (Fig. 4) that more closely approximate the archetypical metal-on-glass contact mask. This type of divergence leads to a broadening of the putatively exposed area in the resist and reveals the failure of more ordinary contact lithographies with light as the feature size shrinks to that of the wavelength.

Fig. 5 shows the energy flow in a structure that combines both lateral air gaps and thin metallic adsorbers. Particularly striking here is the fast decay in the intensity of the field below the gaps in the LCM, leading to a significantly reduced background compared to the case shown in Fig. 2. The intensity transmitted through the mask into the resist is somewhat smaller than in the case without metalization (Fig. 2), although the field coupled into the photoresist remains well focused below the contacting area.

This paper illustrated the contribution of the various building blocks of an LCM to the focusing and guiding of light propagating through it. In addition to improving our understanding of the interaction of light with mesoscopic systems comprising heterogeneous materials, the calculations presented here should provide useful guidance in the further development of this new optical lithography technique.

We thank R. Vahldieck (ETH) and P. Guéret (IBM) for their support of this project. O.J.F.M. gratefully acknowledges the funding of the Swiss National Science Foundation.

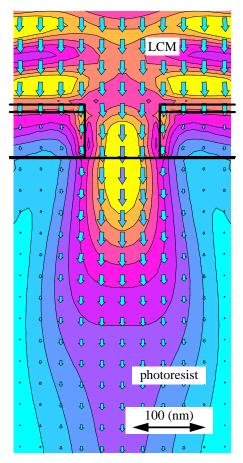


Fig. 5. Light propagation through an LCM where the protrusion is defined by a 60-nm-thick air gap with a 10-nm gold metal layer. The figure shows the field intensity map and the Quicktime movie an animation of the field propagation in the structure (evolution of the electric field amplitude as a function of time; each frame represents a 10° change in the phase of the field). The arrows represent the time-averaged Poynting vector.